



STIX imaging tutorial



Paolo Massa

Department of Physics and Astronomy, Western Kentucky University



Joint work with: Volpara A., Battaglia A. F., Perracchione E., Garbarino S., Benvenuto F., Massone A. M., Hurford G. J., Piana M., Krucker S.
& the STIX team

n|w

July 14, 2022, SPHERE workshop 2022

WKU

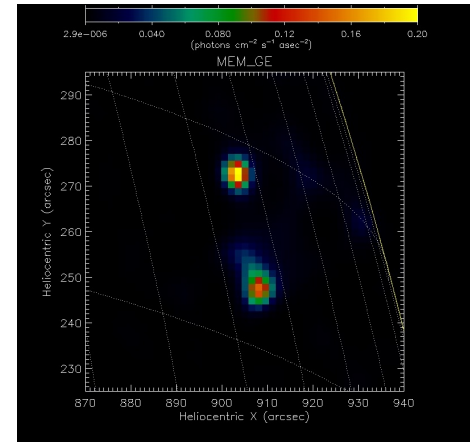
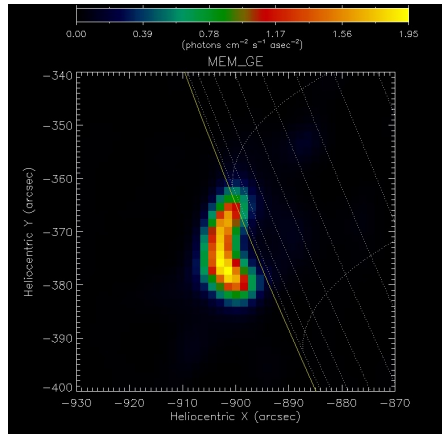
The STIX instrument

STIX imaging objective:

reconstruct the image of the flaring X-ray emission from indirect measurements

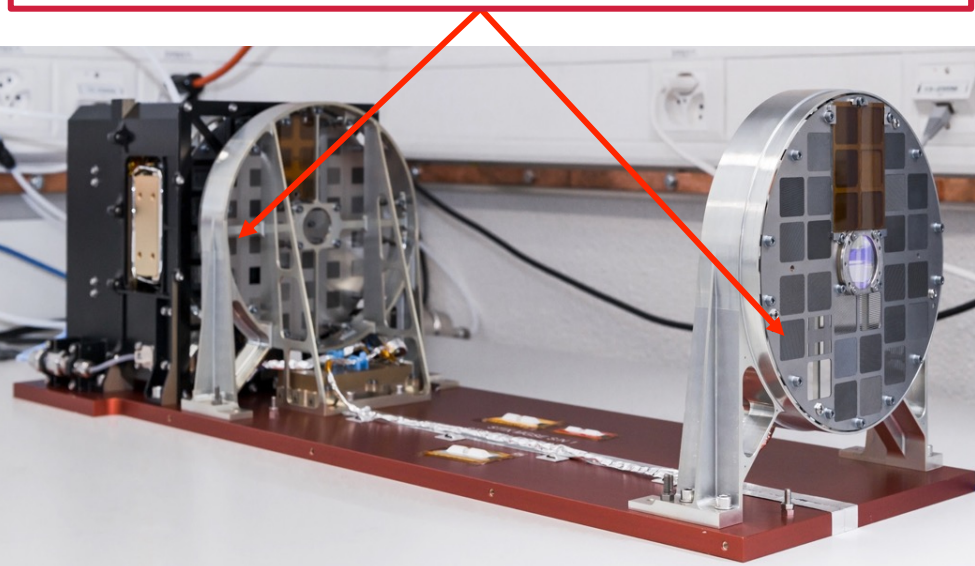
Fourier components of the angular distribution of the X-ray source

Examples from RHESSI data (Lin et al., 2002)



The STIX instrument

Subcollimator = front grid + rear grid + detector



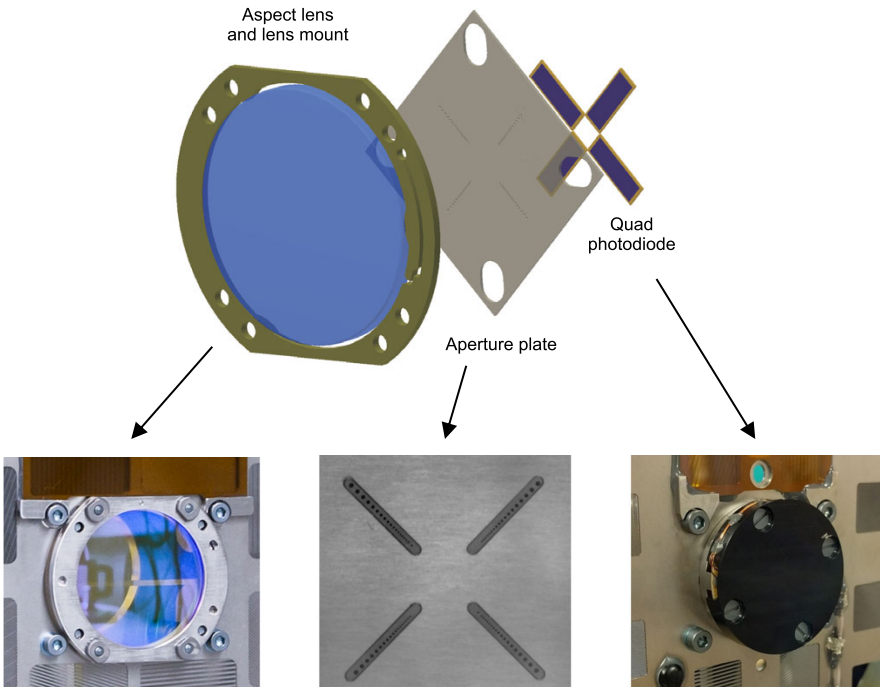
Krucker et al., 2020

Bigrid imaging system

STIX consists of 32 subcollimators:

- 30 are used for imaging
- Coarse Flare Locator
- Background monitor

The STIX instrument

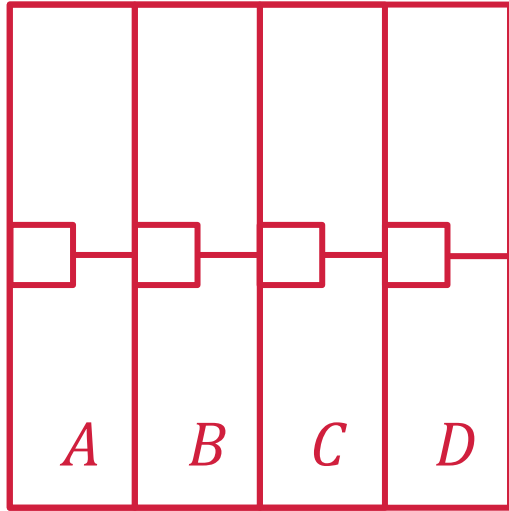


Warmuth et al., 2020

STIX Aspect System (SAS)

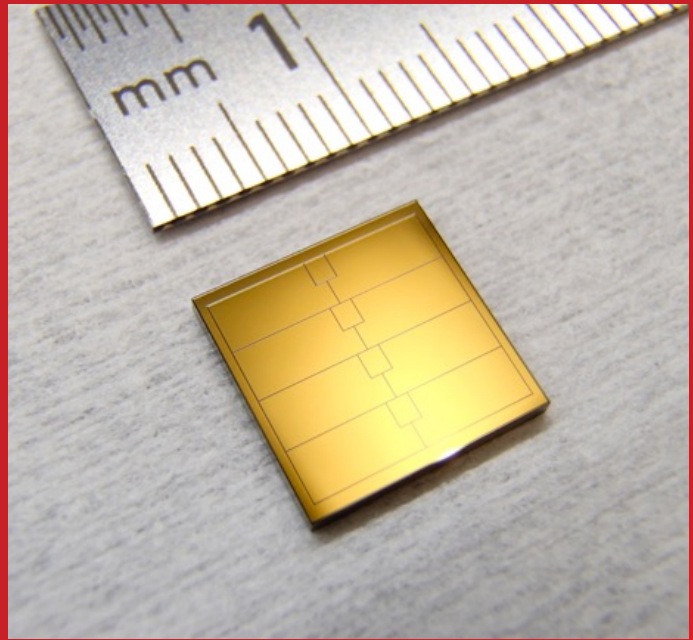
- Optical (aspect) lens imaging the Sun
- Aperture plate in the rear grid (cross-shaped configuration)
- Photodiodes record light passing through the apertures
- Variation of the STIX pointing are detected
- SAS solution available when the distance between SolO and the Sun is less than 0.75 AU

The STIX instrument



A, B, C and D: number of counts recorded by the detector pixels

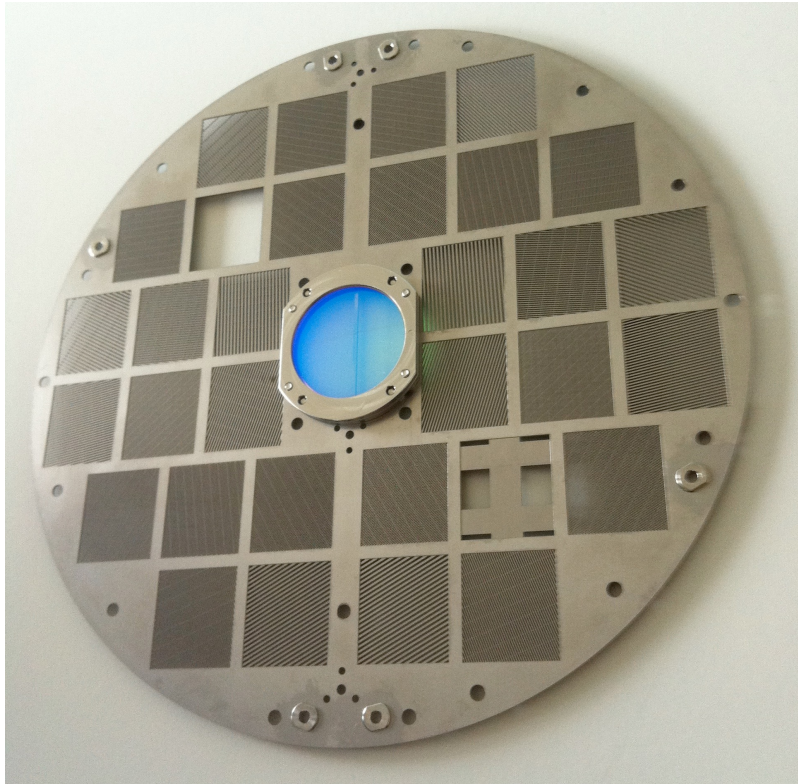
STIX Cadmium-Telluride detector
(Meuris et al. 2015)



Krucker et al., 2020

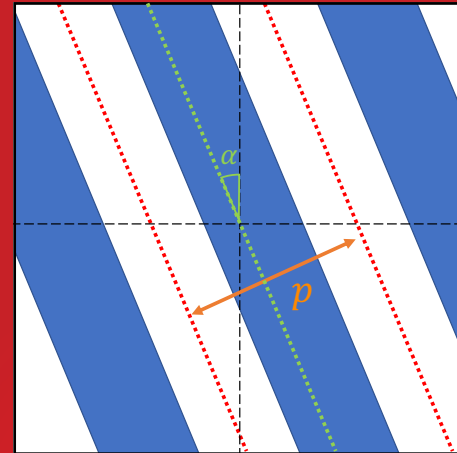
WKU®

The STIX instrument



Grid parameters:

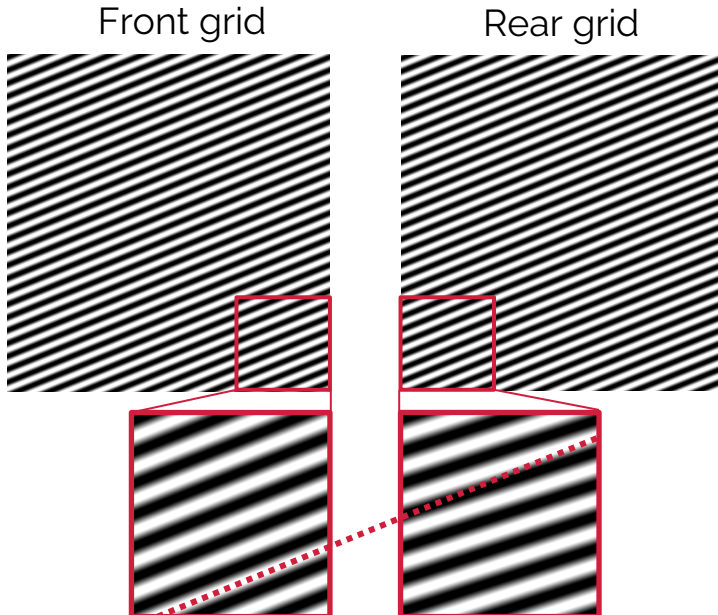
- α : orientation angle
- p : pitch = distance between two consecutive slit centers



WKU®

The STIX imaging concept

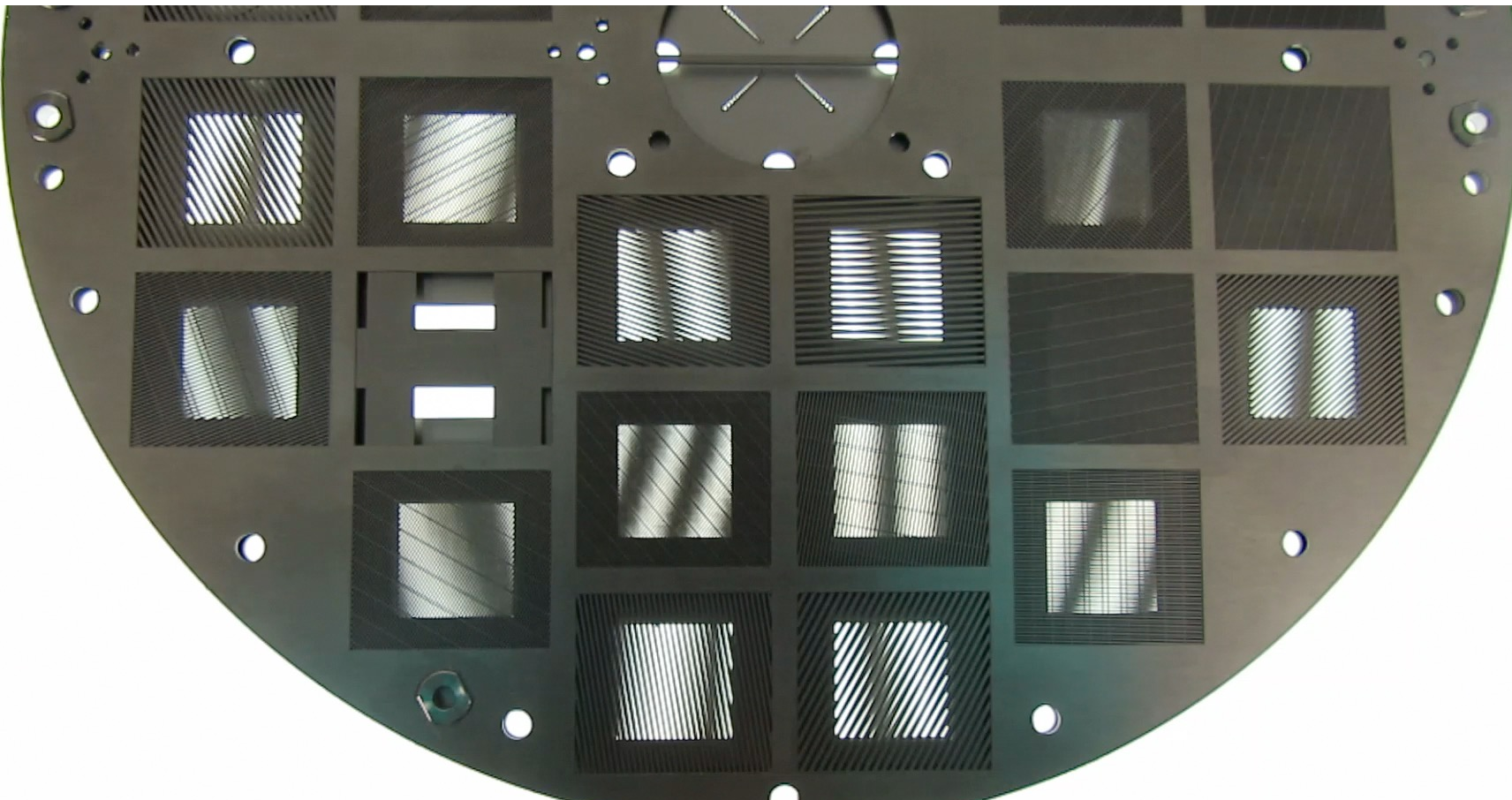
Front and rear grid have different orientation and pitch



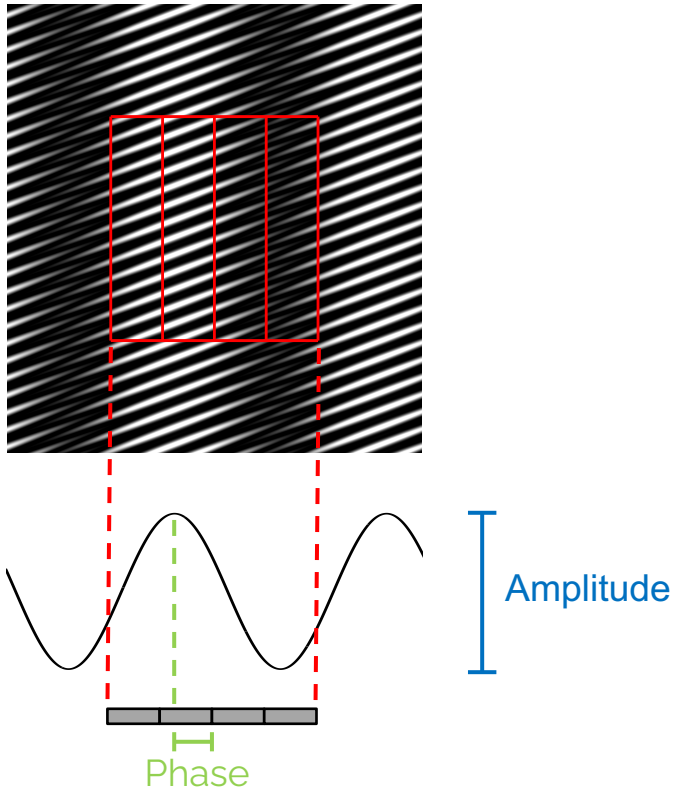
The transmitted X-ray photon flux creates a **Moiré pattern**



The STIX imaging concept



The STIX imaging concept



Moiré patterns have:

- period equal to the detector width
- orientation perpendicular to the pixels stripes

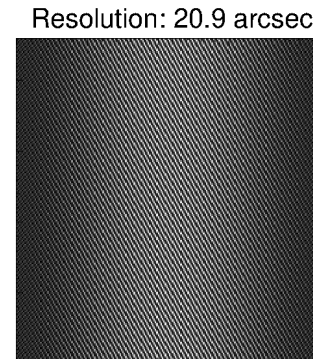
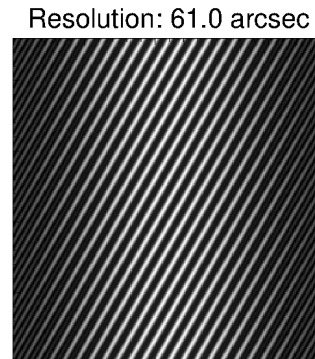
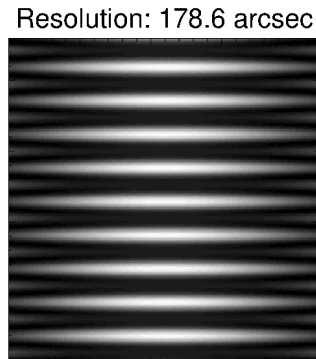
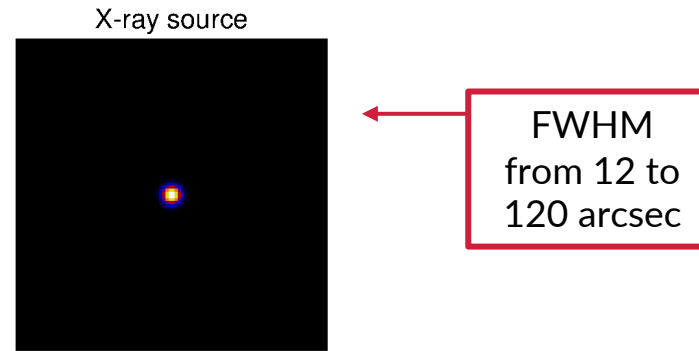
Amplitude and phase of a pattern



Amplitude and phase of a Fourier component of the X-ray source

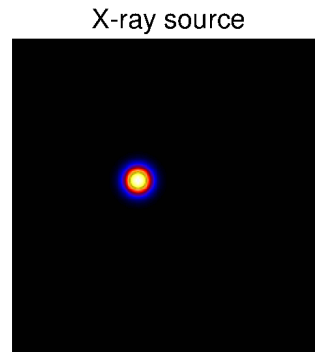
The STIX imaging concept

The amplitude of a Moiré pattern is sensitive to the source size

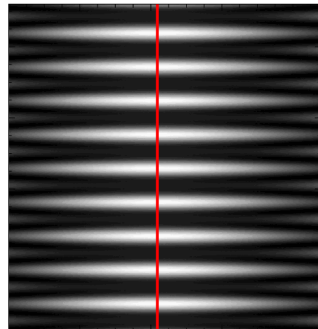


The STIX imaging concept

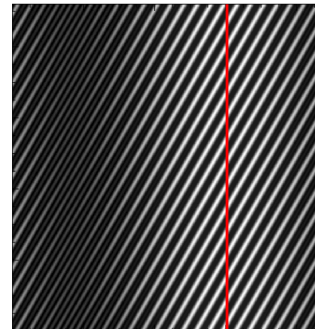
The phase of a Moiré pattern is sensitive to the source location



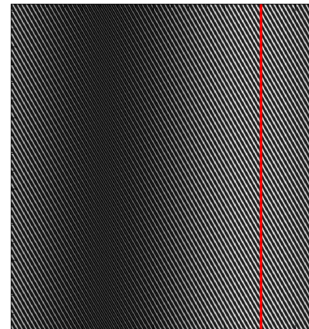
Resolution: 178.6 arcsec



Resolution: 61.0 arcsec



Resolution: 20.9 arcsec



The STIX imaging concept

$\phi(x, y)$ represents the intensity of the X-ray radiation emitted from (x, y) on the Sun disk

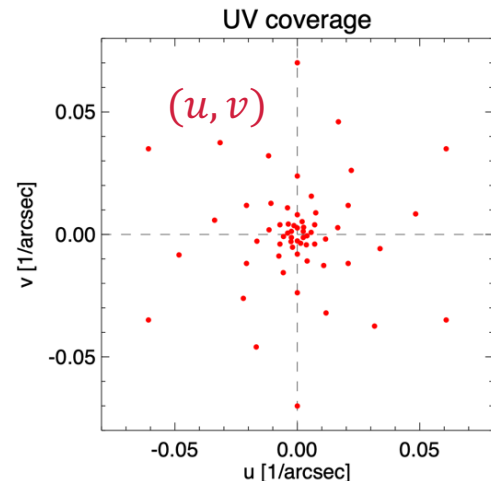
Data measured by STIX: $\mathbf{V} = (V_1, \dots, V_{30})$, where

$$V = \iint \phi(x, y) \exp(2\pi i(xu + yv)) dx dy$$

- $|V| \propto \sqrt{(C - A)^2 + (D - B)^2}$
- $\phi = \text{atan}\left(\frac{D-B}{C-A}\right) + 45^\circ + \phi_{\text{calib}}$

Determined by count measurements

Krucker et al., 2020



Determined by grids' pitch and orientation

The STIX imaging concept

$\phi(x, y)$ represents the intensity of the X-ray radiation emitted from (x, y) on the Sun disk

Data measured by STIX: $\mathbf{V} = (V_1, \dots, V_{30})$, where

$$V = \iint \phi(x, y) \exp(2\pi i(xu + yv)) dx dy$$

Image reconstruction problem for STIX: determine ϕ s.t.

$$\mathbf{F}\phi = \mathbf{V}$$

where \mathbf{F} is the Fourier transform computed in the STIX frequencies

Imaging methods

Imaging methods

- Back-projection (Mertz et al., 1986)
- Clean (Högbom, 1974)
- MEM_GE (Massa et al., 2020)
- EM (Massa et al., 2019)
- VIS_FWDFIT_PSO (Volpara et al., in preparation)

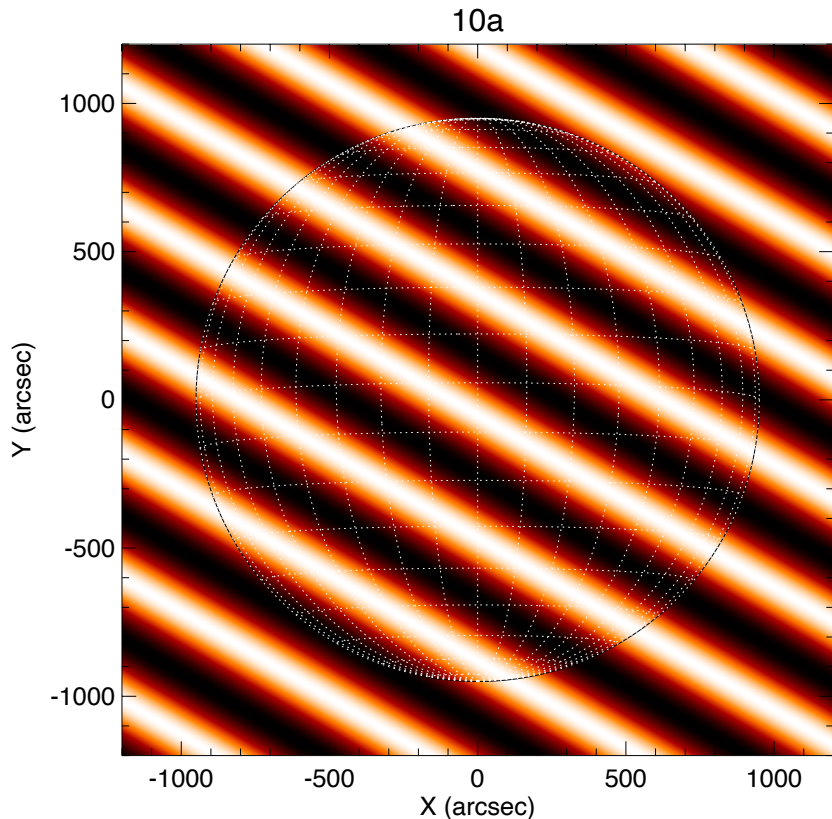
+

Other methods in preparation:

- UV_SMOOTH (Perracchione et al, 2021)
- Sequential Monte Carlo (SMC, Sciacchitano et al., 2018)
- ...

- **The STIX imaging problem has no unique solution**
- Need to develop many different algorithms and compare their results
- RHESSI legacy: we can use the same algorithms

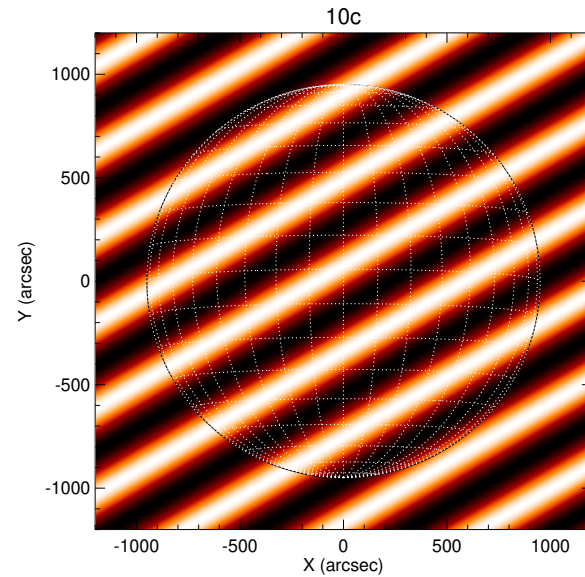
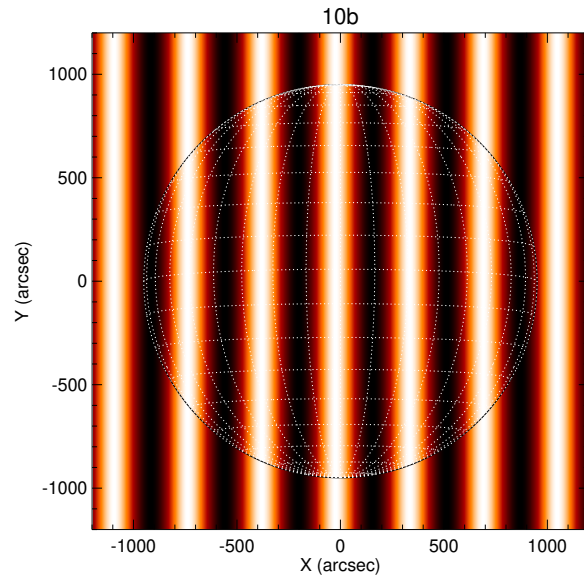
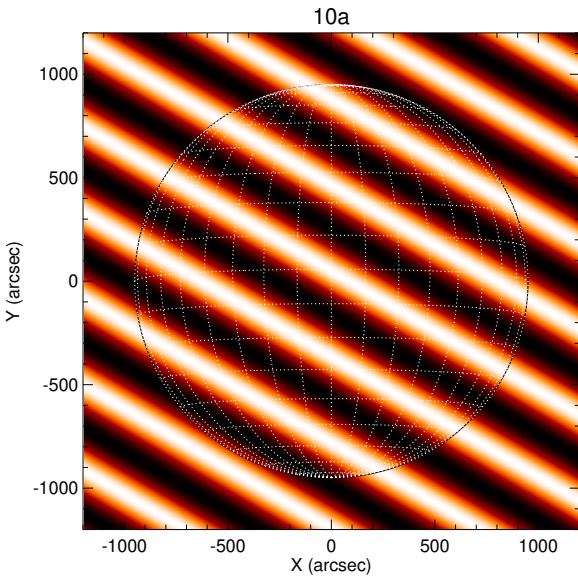
Back-projection



- Direct Fourier inversion
- Idea: the Back Projection of a single visibility is a sinusoidal wave

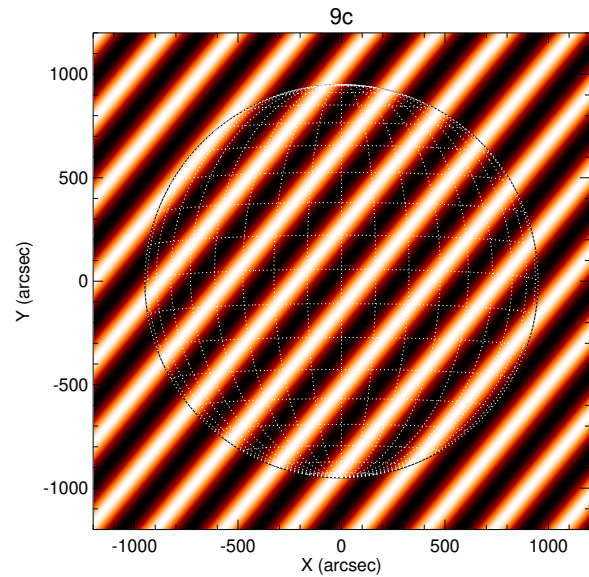
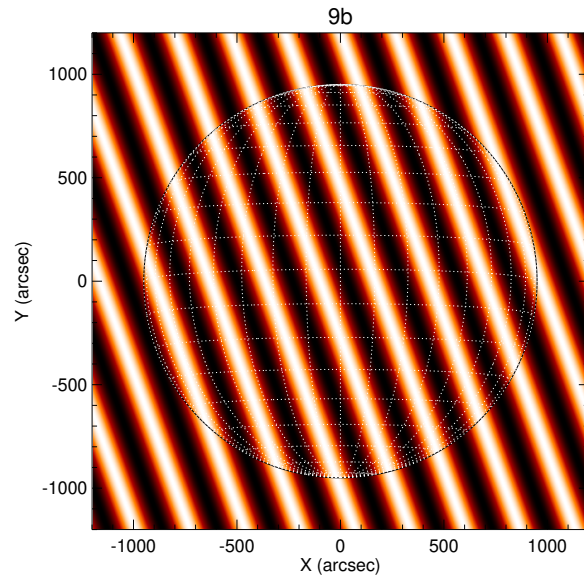
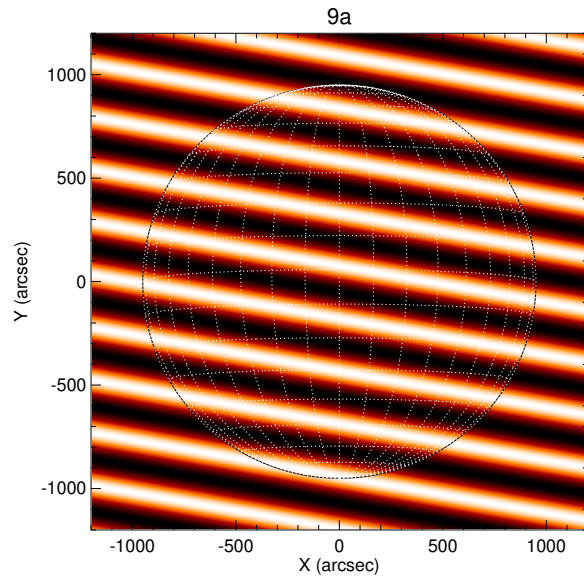
Back-projection

Detectors with the same resolution produce waves with same period but different orientation



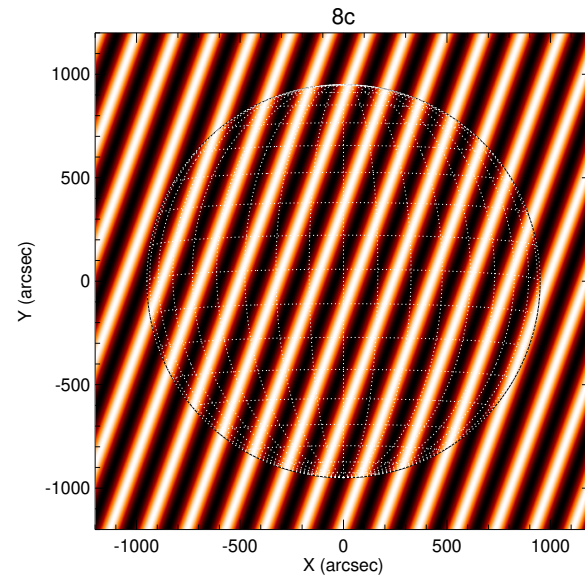
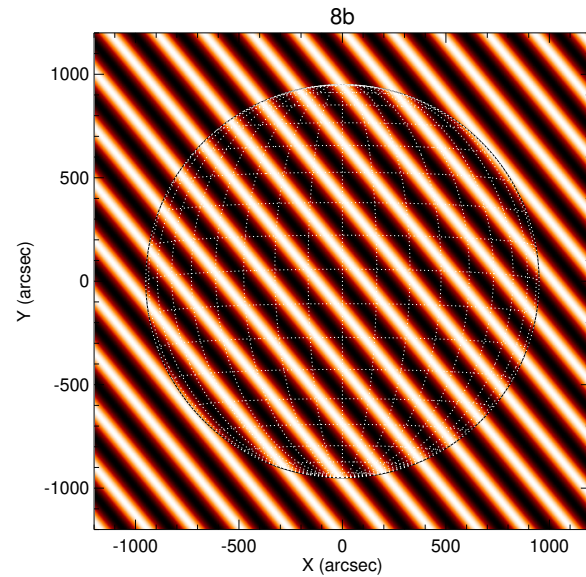
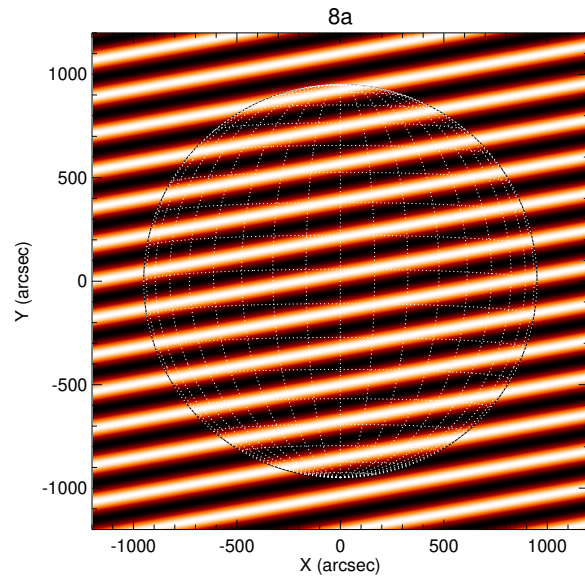
Back-projection

Detectors with the same resolution produce waves with same period but different orientation

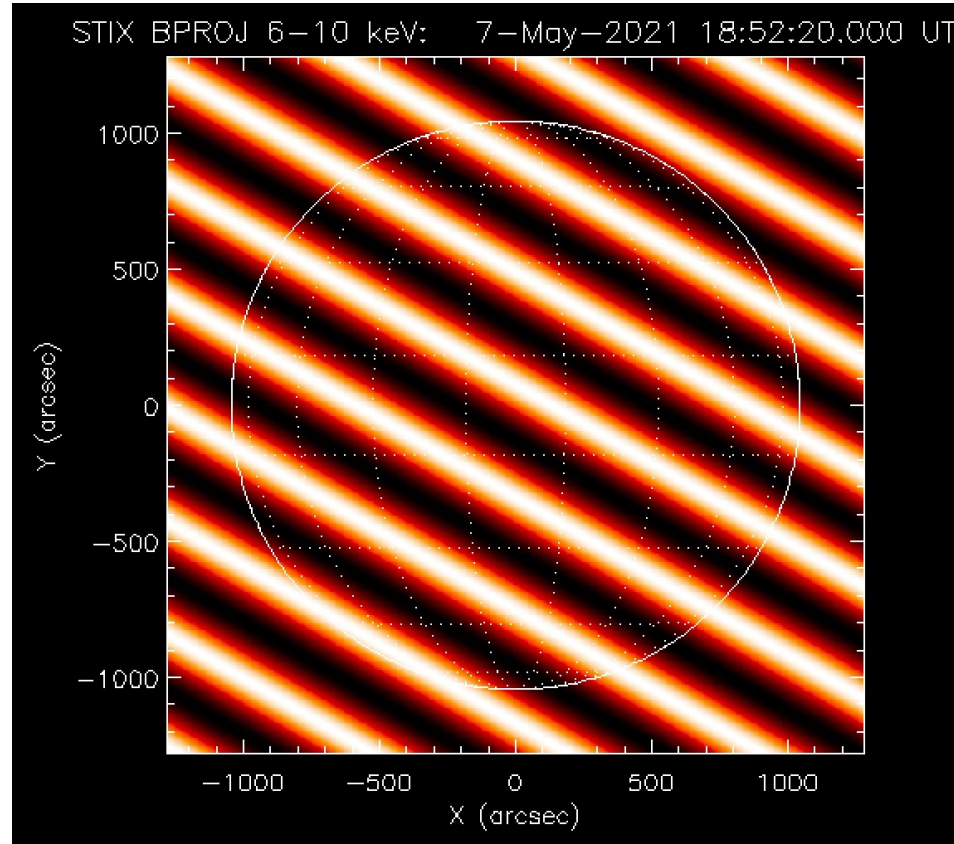


Back-projection

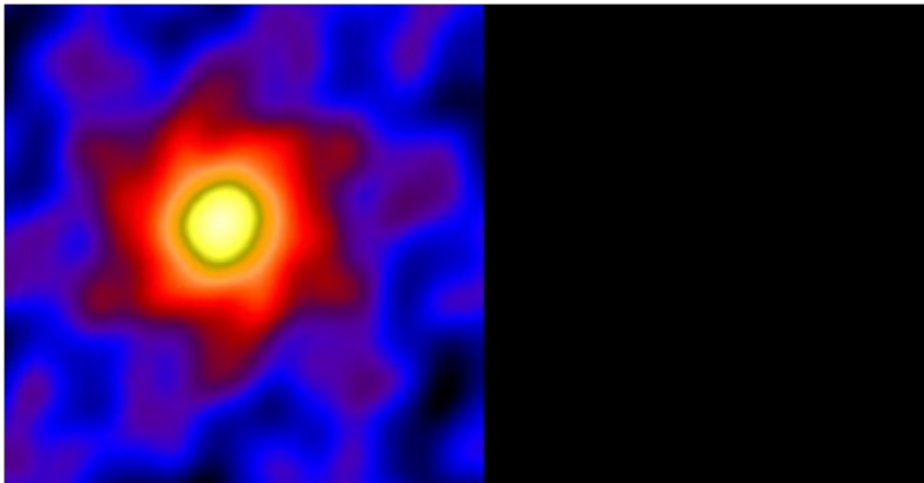
Detectors with the same resolution produce waves with same period but different orientation



Back-projection



Clean

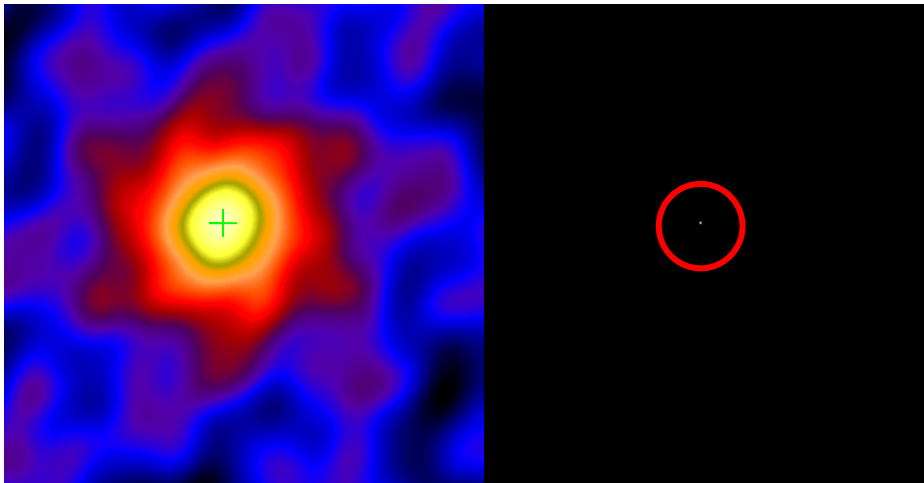


Iterative method:

- Creates two maps: **dirty map** (back projection) and **clean components (cc) map** (zero map)



Clean

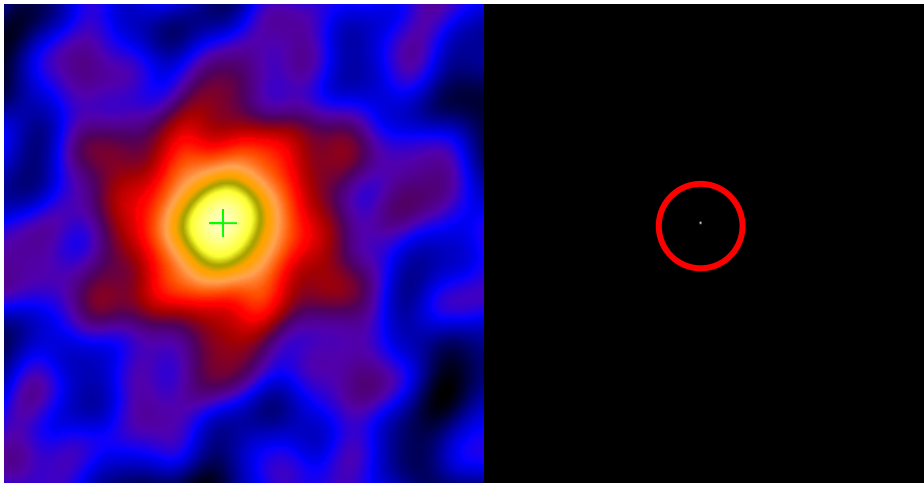


Iterative method:

- Creates two maps: **dirty map** (back projection) and **clean components (cc) map** (zero map)
- Finds maximum of the dirty map and add clean component in the cc map

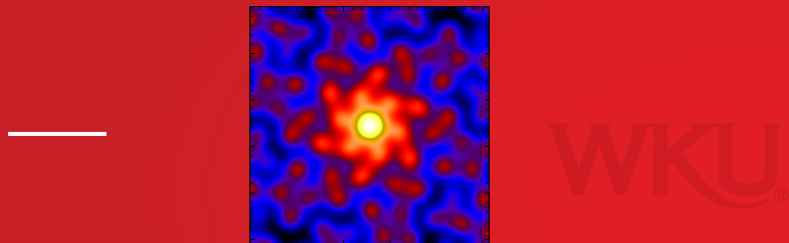
—

Clean

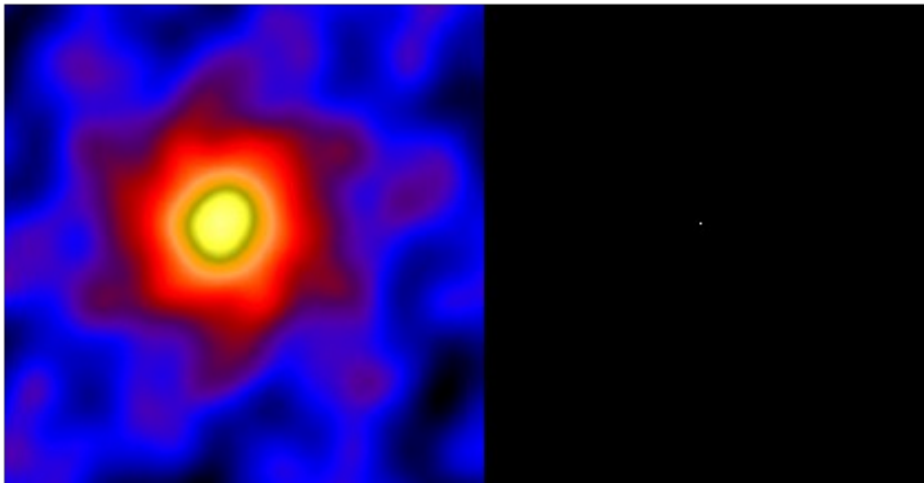


Iterative method:

- Creates two maps: **dirty map** (back projection) and **clean components (cc) map** (zero map)
- Finds maximum of the dirty map and add clean component in the cc map
- Subtracts a fraction of the PSF from the dirty map



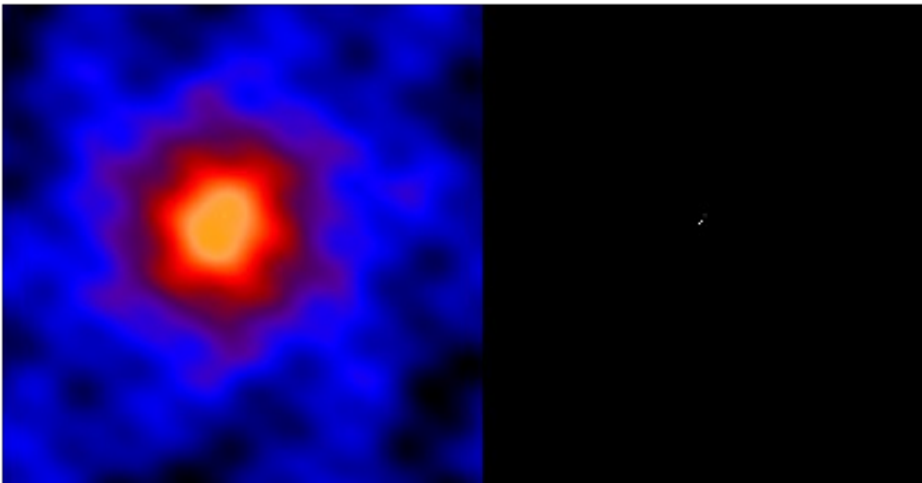
Clean



Iterative method:

- Creates two maps: **dirty map** (back projection) and **clean components (cc) map** (zero map)
- Finds maximum of the dirty map and add clean component in the cc map
- Subtracts a fraction of the PSF from the dirty map
- Iterates

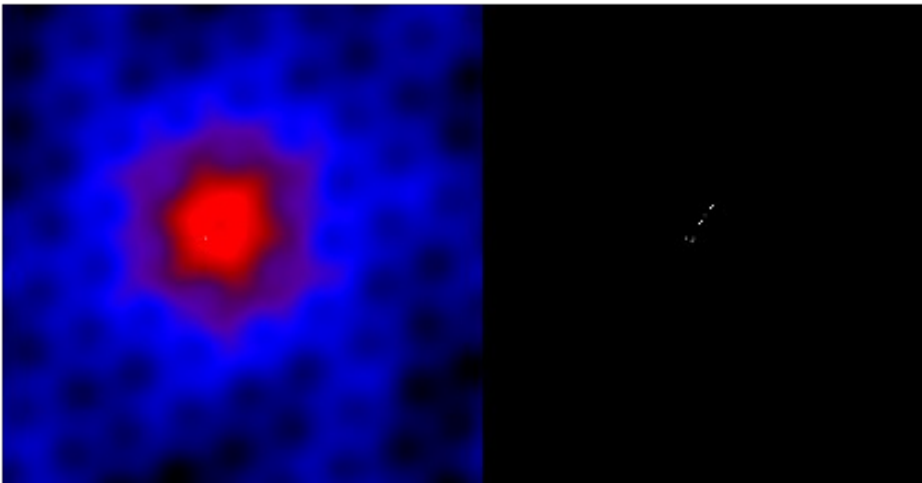
Clean



Iterative method:

- Creates two maps: **dirty map** (back projection) and **clean components (cc) map** (zero map)
- Finds maximum of the dirty map and add clean component in the cc map
- Subtracts a fraction of the PSF from the dirty map
- Iterates

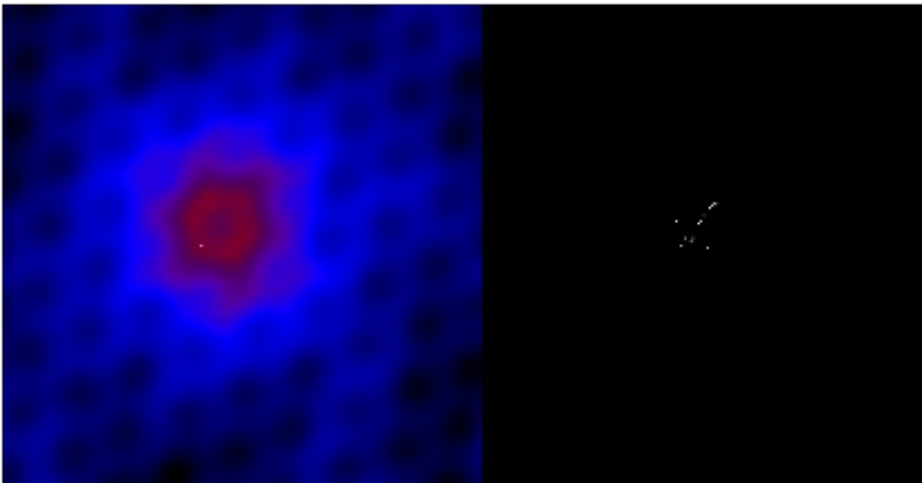
Clean



Iterative method:

- Creates two maps: **dirty map** (back projection) and **clean components (cc) map** (zero map)
- Finds maximum of the dirty map and add clean component in the cc map
- Subtracts a fraction of the PSF from the dirty map
- Iterates

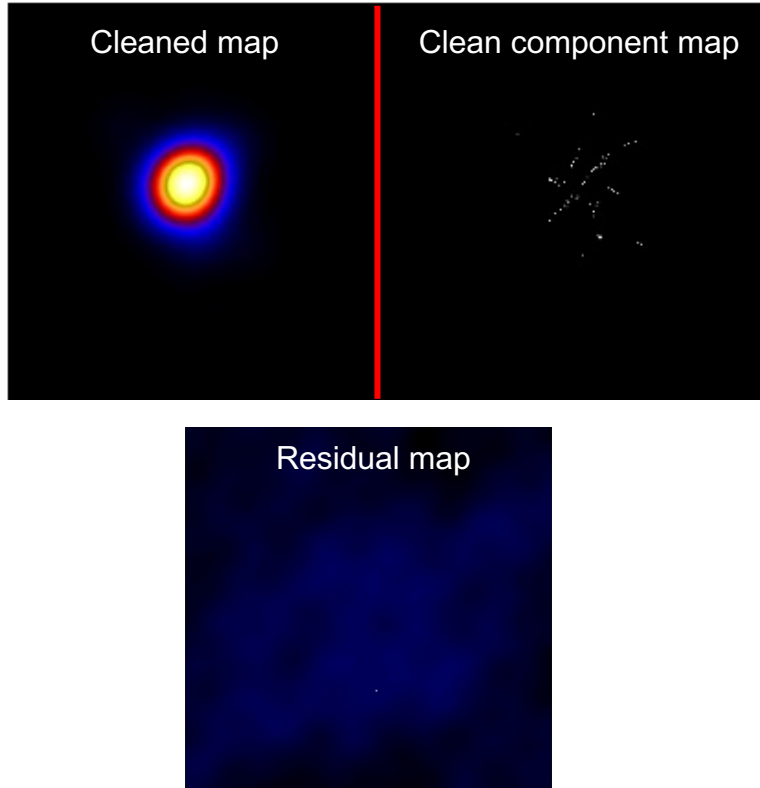
Clean



Iterative method:

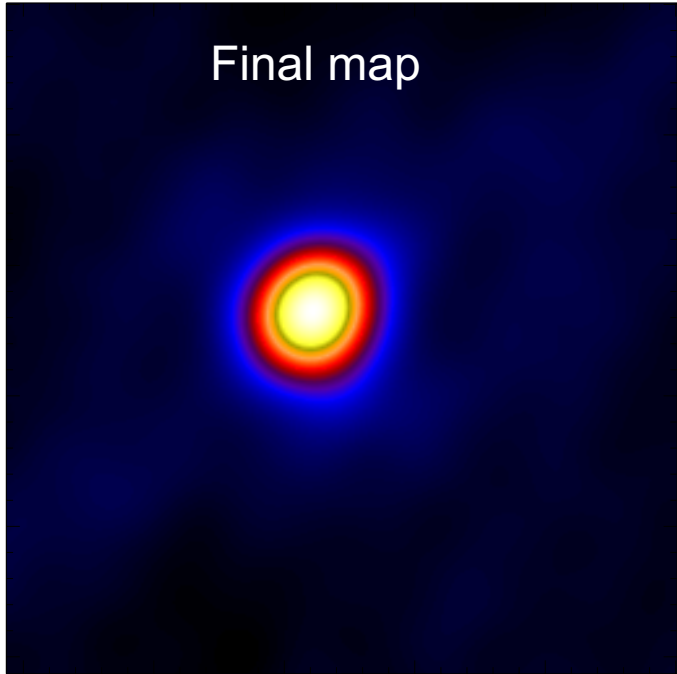
- Creates two maps: **dirty map** (back projection) and **clean components (cc) map** (zero map)
- Finds maximum of the dirty map and add clean component in the cc map
- Subtracts a fraction of the PSF from the dirty map
- Iterates

Clean



Final step: convolution with
clean beam and residuals

Clean



Final step: convolution with
clean beam and residuals

MEM_GE

Solves the maximum-entropy regularized problem:

$$\arg \min_{\phi \geq 0} \chi^2(\phi) - \lambda H(\phi)$$

$$\text{with } \sum_j \phi_j = f$$

where

$$\chi^2(\phi) = \sum_i \frac{|(\mathcal{F}\phi)_i - V_i|^2}{\sigma_i^2} \quad H(\phi) = - \sum_j \phi_j \log \left(\frac{\phi_j}{me} \right)$$

MEM_GE

Solves the maximum-entropy regularized problem:

$$\arg \min_{\phi \geq 0} \chi^2(\phi) - \lambda H(\phi)$$

with $\sum_j \phi_j = f$

where

$$\chi^2(\phi) = \sum_i \frac{|(\mathcal{F}\phi)_i - V_i|^2}{\sigma_i^2}$$

$$H(\phi) = - \sum_j \phi_j \log \left(\frac{\phi_j}{m e} \right)$$

Data fitting

MEM_GE

Solves the maximum-entropy regularized problem:

$$\arg \min_{\phi \geq 0} \chi^2(\phi) - \lambda H(\phi)$$

$$\text{with } \sum_j \phi_j = f$$

where

$$\chi^2(\phi) = \sum_i \frac{|(\mathcal{F}\phi)_i - V_i|^2}{\sigma_i^2}$$

$$H(\phi) = - \sum_j \phi_j \log \left(\frac{\phi_j}{me} \right)$$

Regularization

MEM_GE

Solves the maximum-entropy regularized problem:

$$\arg \min_{\phi \geq 0} \chi^2(\phi) - \lambda H(\phi)$$

$$\text{with } \sum_j \phi_j = f$$

Regularization
parameter

where

$$\chi^2(\phi) = \sum_i \frac{|(\mathcal{F}\phi)_i - V_i|^2}{\sigma_i^2}$$

$$H(\phi) = - \sum_j \phi_j \log \left(\frac{\phi_j}{me} \right)$$

MEM_GE

Solves the maximum-entropy regularized problem:

Positivity constraint $\xrightarrow{\phi \geq 0}$
$$\arg \min \chi^2(\phi) - \lambda H(\phi)$$

with
$$\sum_j \phi_j = f$$

where

$$\chi^2(\phi) = \sum_i \frac{|(\mathcal{F}\phi)_i - V_i|^2}{\sigma_i^2} \quad H(\phi) = - \sum_j \phi_j \log \left(\frac{\phi_j}{me} \right)$$

MEM_GE

Solves the maximum-entropy regularized problem:

$$\arg \min_{\phi \geq 0} \chi^2(\phi) - \lambda H(\phi)$$

with $\sum_j \phi_j = f$ ← Flux constraint

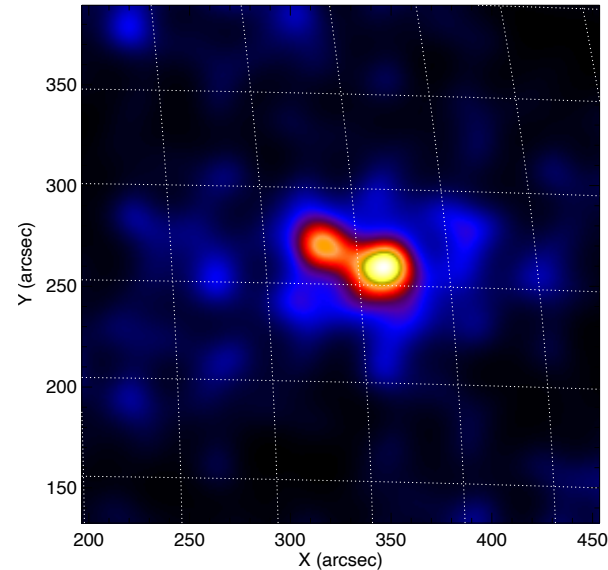
where

$$\chi^2(\phi) = \sum_i \frac{|(\mathcal{F}\phi)_i - V_i|^2}{\sigma_i^2} \quad H(\phi) = - \sum_j \phi_j \log \left(\frac{\phi_j}{m e} \right)$$

MEM_GE

λ finds tradeoff between data fitting and regularization:

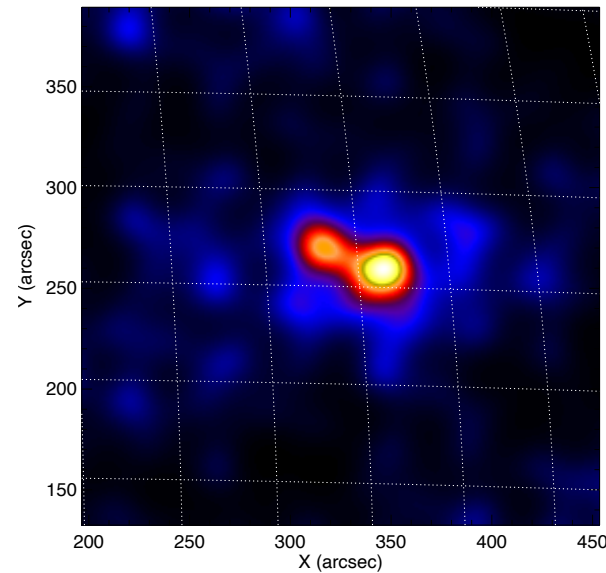
Large λ



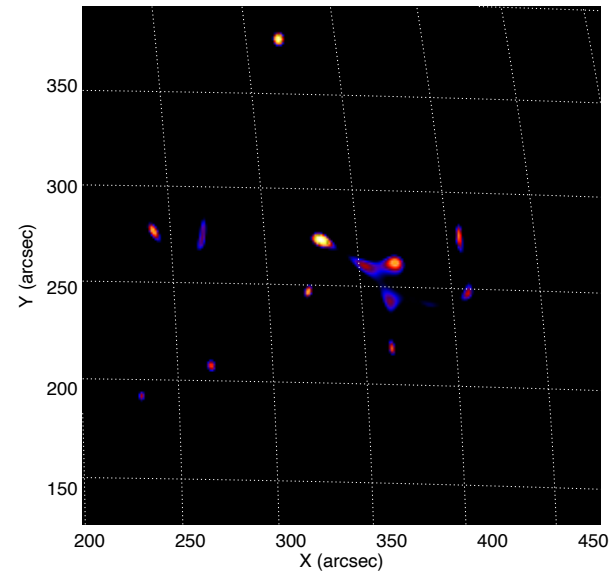
MEM_GE

λ finds tradeoff between data fitting and regularization:

Large λ



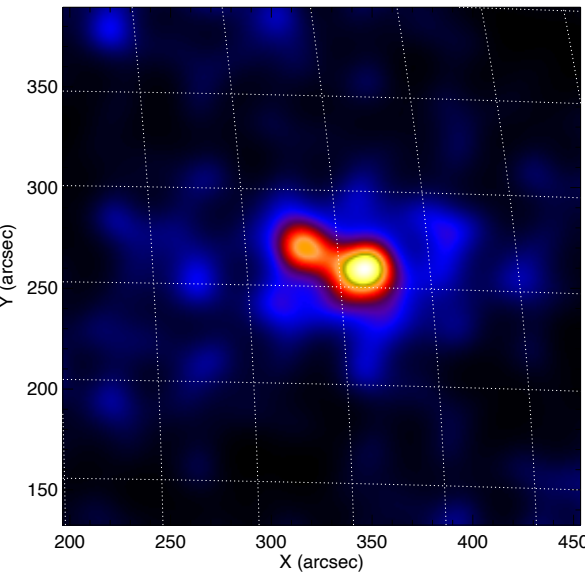
Low λ



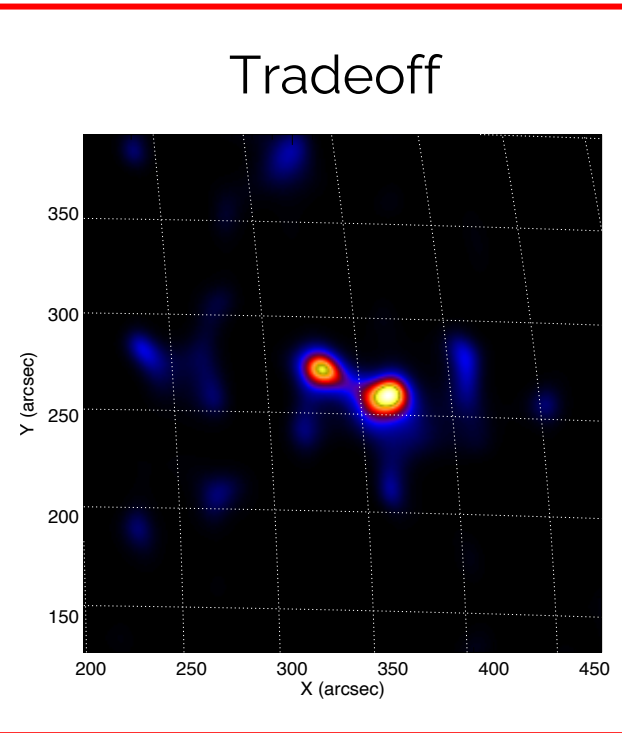
MEM_GE

λ finds tradeoff between data fitting and regularization:

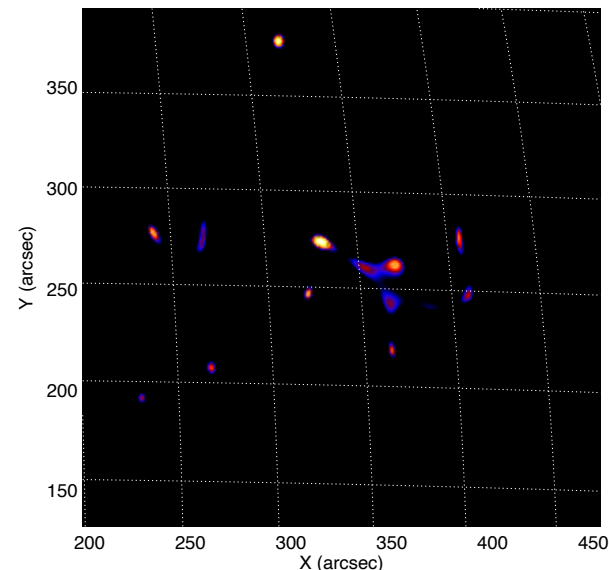
Large λ



Tradeoff



Low λ



Expectation Maximization

- Count based method which solves

$$M\phi = \mathbf{C}$$

Expectation Maximization

- Count based method which solves

$$M\phi = \mathbf{C}$$

Matrix modeling the grids' transmission

Expectation Maximization

- Count based method which solves

$$M\phi = \mathbf{C}$$

Array containing the measured counts

Expectation Maximization

- Count based method which solves

$$M\phi = \mathbf{C}$$

- Maximum likelihood approach:

$$\arg \max_{\phi \geq 0} P(\mathbf{C}|\phi)$$

Expectation Maximization

- Count based method which solves

$$M\phi = \mathbf{C}$$

- Maximum likelihood approach:

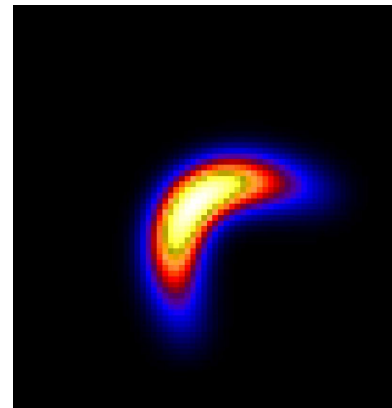
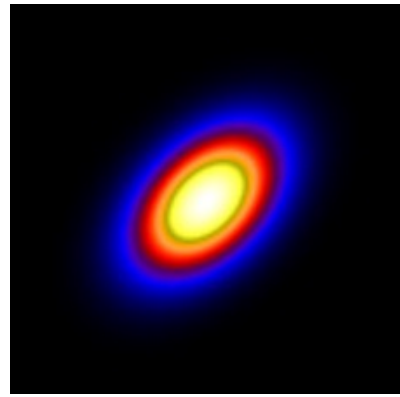
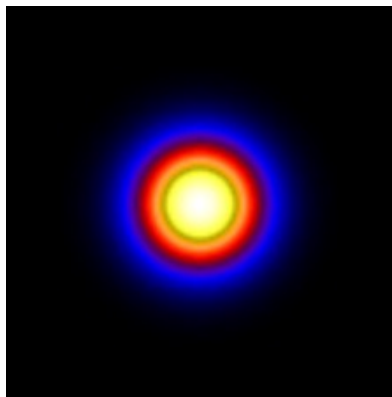
$$\arg \max_{\phi \geq 0} P(\mathbf{C}|\phi)$$

- Same as Richardson-Lucy:

$$\phi_{k+1} = \frac{\phi_k}{M^T 1} M^T \left(\frac{\mathbf{C}}{M\phi_k} \right)$$

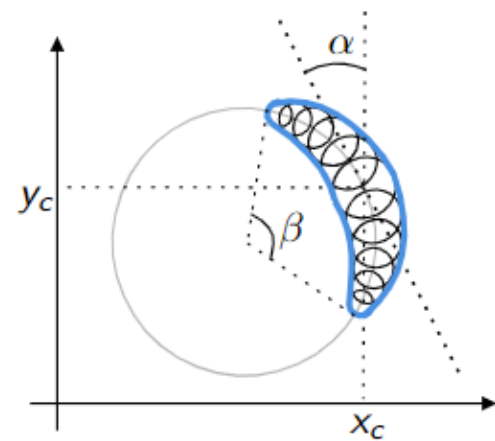
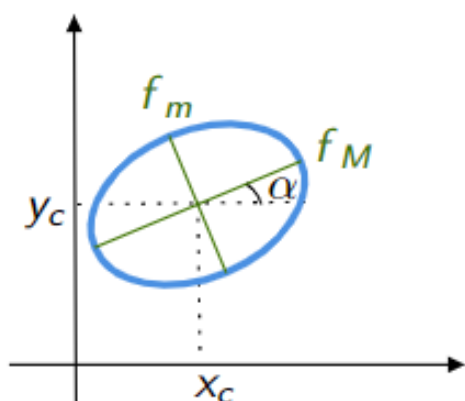
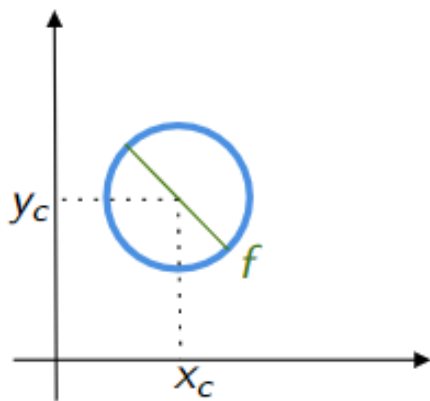
VIS_FWDFIT_PSO

- Parametric imaging
- Choose a parametric shape ϕ_θ among



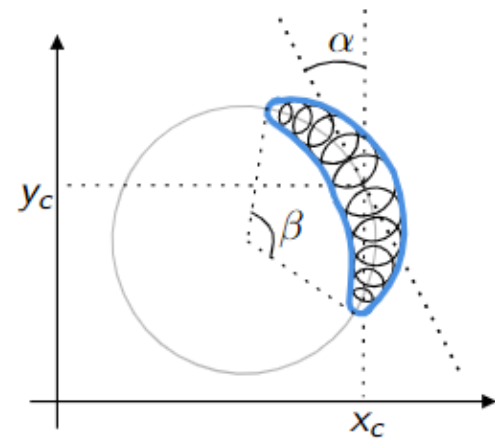
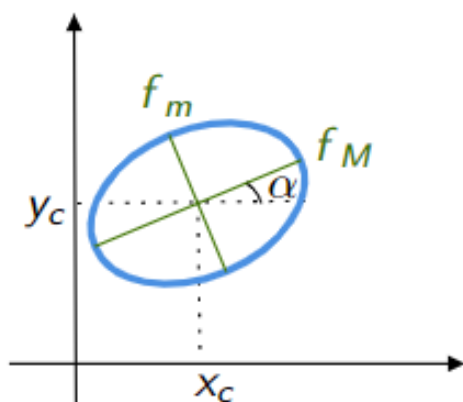
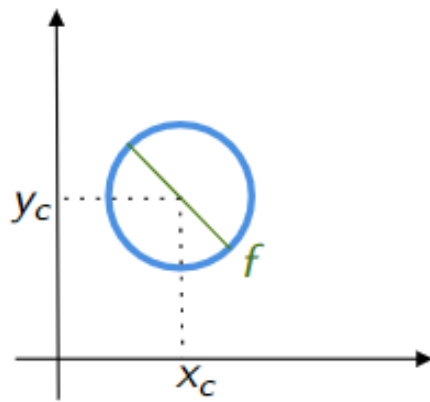
VIS_FWDFIT_PSO

- Parametric imaging
- Choose a parametric shape ϕ_θ among



VIS_FWDFIT_PSO

- Parametric imaging
- Choose a parametric shape ϕ_θ among

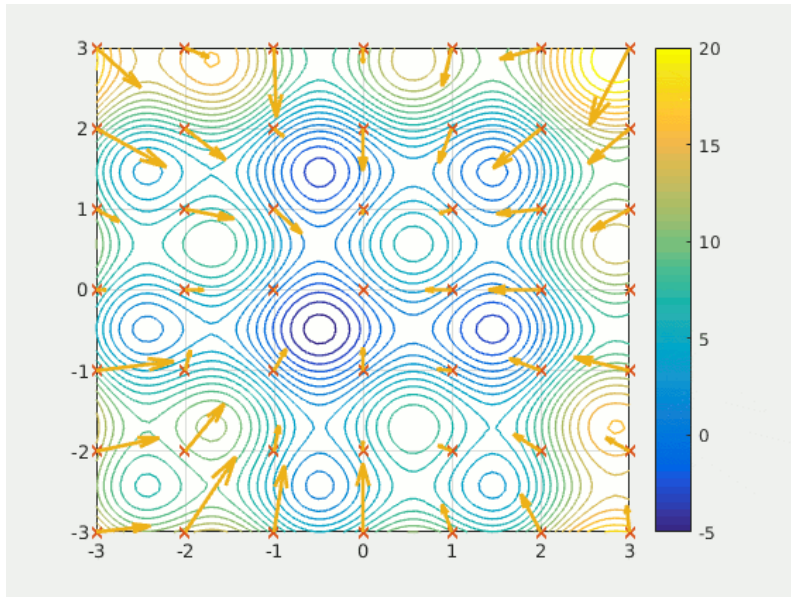


- Solve

$$\theta^* = \operatorname{argmin}_\theta \frac{1}{N_V - N_{\phi_\theta}} \sum_i \frac{|(F\phi_\theta)_i - V_i|^2}{\sigma_i^2}$$

VIS_FWDFIT_PSO

- **Uncertainty on the parameters:** 20 reconstructions from visibilities perturbed with Gaussian noise and computation of the standard deviation
- **New optimization method:** based on Particle Swarm Optimization (PSO, Eberhart et al., 1995)



By Ephramac - Own work, CC BY-SA 4.0,
<https://commons.wikimedia.org/w/index.php?curid=54975083>

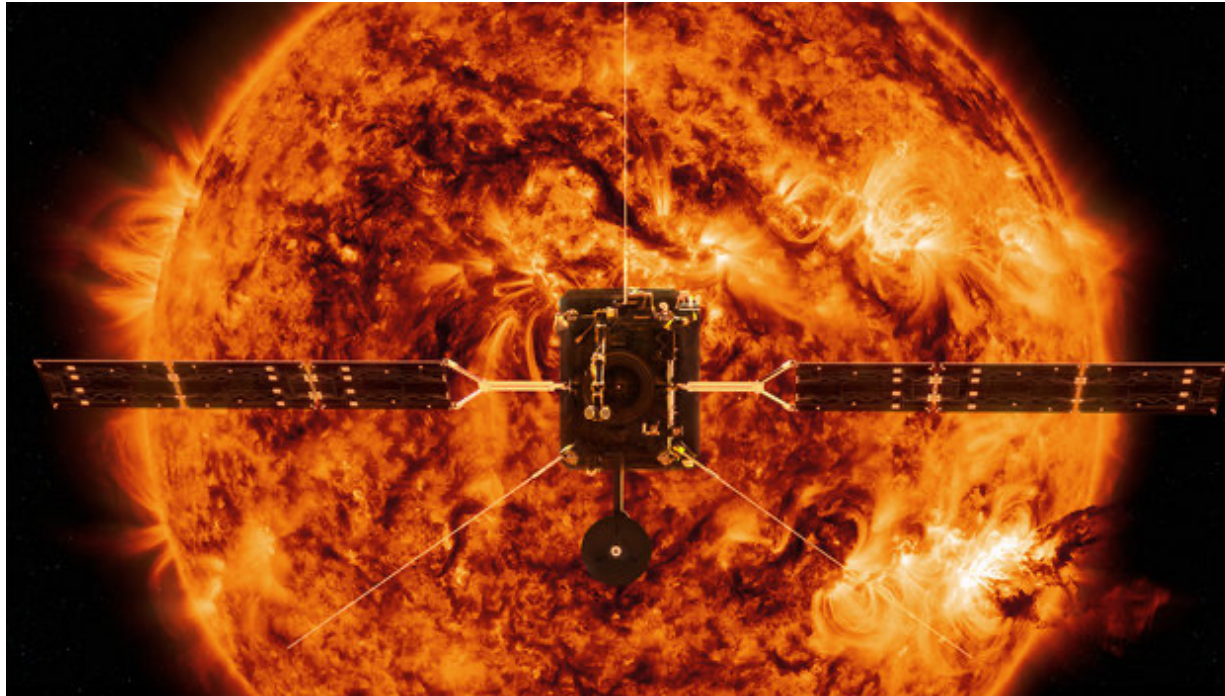
STIX imaging status

- Reached a satisfactory level for scientific data exploitation
- Absolute location of STIX reconstructions to be improved (to reach goal of 4 arcsec precision)
- Calibration of the finest resolution detectors to be investigated
- Second order errors in data calibration to be corrected

References

- Battaglia et al., *STIX X-ray microflare observations during the Solar Orbiter commissioning phase*, A&A, 2021
- Högbom, *Aperture synthesis with a non-regular distribution of interferometer baselines*, Astronomy and Astrophysics Supplement, 1974
- Hurford et al, *The RHESSI imaging concept*, Solar Physics, 2002
- Krucker et al., *The Spectrometer/Telescope for Imaging X-rays (STIX)*, A&A, 2020
- Lin et al. , *The Reuven Ramaty High-Energy Solar Spectroscopic Imager (RHESSI)*, Solar Physics, 2002
- Massa et al., *Count-based imaging model for the Spectrometer/Telescope for Imaging X-rays (STIX) in Solar Orbiter*, A&A, 2019
- Massa et al., *MEM_GE: A New Maximum Entropy Method for Image Reconstruction from Solar X-Ray Visibilities*, APJ, 2020
- Massa et al., *Imaging from STIX visibility amplitudes*, A&A, 2021
- Massa et al., *First hard X-ray imaging results by Solar Orbiter STIX*, accepted for publication in Solar Physics, 2022
- Mertz et al., *Rotational aperture synthesis for x rays*, JOSA A, 1986
- Meuris et al., *Caliste-SO, a CdTe based spectrometer for bright solar event observations in hard X-rays*, Nucl. Instrum. Methods Phys. Res. A, 2015

Thanks for the attention!



If you have questions, write me at: paolo.massa@wku.edu